

# Green synthesis of gold nanoparticles using aqueous *Aegle marmelos* leaf extract and their application for thiamine detection†

Cite this: *RSC Adv.*, 2014, 4, 28645

K. Jagajjanani Rao and Santanu Paria\*

Nanoparticles of noble metals, especially gold nanoparticles are studied extensively because of their new and amazing properties. Among several synthesis techniques, green synthesis of nanoparticles is promising in recent years. In this study, we investigated the potential of *Aegle marmelos* leaf extract (LE) in reduction of  $\text{HAuCl}_4$  to form  $\sim 38.2 \pm 10.5$  nm spherical shape polyphenol capped gold nanoparticles. The stoichiometric proportion of the LE to  $\text{HAuCl}_4$  and the equilibrium time to complete the reduction process for the nanoparticle formation were also identified. The total reaction time was observed to be within  $\sim 30$  min from the particle formation kinetics study. The as-synthesized gold nanoparticles capped with polyphenols of leaf extract were shown to be very effective for the detection of vitamin B and thiamine to a minimum concentration of  $\sim 0.5$   $\mu\text{M}$ .

Received 28th April 2014  
Accepted 18th June 2014

DOI: 10.1039/c4ra03883e

[www.rsc.org/advances](http://www.rsc.org/advances)

## 1 Introduction

Synthesis of nanoparticles (NPs) using green processes is receiving immense attention in recent years over the conventional bottom-up chemical routes, because of several advantages of green routes such as environmental friendliness, use of renewable natural resources, more bio-compatible nature for biological applications.<sup>1,2</sup> Among the available green methodologies, biosynthesis of nanoparticles has attracted greater attention for its mild reaction conditions, eco-friendly residual products, and *in situ* capping abilities.<sup>2-4</sup> Unlike microbial based synthesis processes, utilization of plant based natural compounds has some advantages such as user friendliness, cost-effectiveness, easy separation and purification processes.<sup>5-7</sup> As a result, various novel nanoparticles have been synthesized by this technique.<sup>6,7</sup>

Among the different NPs, gold (Au) NPs have attracted great attention for their technological and biomedical applications such as diagnostics, biosensors, molecular imaging, drug delivery.<sup>8,9</sup> Numerous studies have also been documented for the phytochemical based synthesis of AuNPs, where the gold ion is reduced by the electron donating plant components or phytochemicals.<sup>10-13</sup> For example, AuNPs from *Chenopodium album* (10–30 nm), geranium leaf (16–40 nm), *Memecylon edule* (20–50 nm), banana peel extract (300 nm), *etc.* are reported before.<sup>14,15</sup> Additionally, few recent studies have also shown the

potential use of the medicinal plants for the synthesis of AuNPs. For example, *Citrus limon* extract was employed to have a 10 nm AuNPs at ambient temperature and neutral pH.<sup>12</sup> Similarly, plant extract from cypress leaves resulted in AuNPs of  $\sim 15$  nm particles within 10 min,<sup>13</sup> active polyphenols and flavonoids of black tea leaf broth gives  $\sim 20$  nm mixed shape AuNPs.<sup>16</sup> Some other therapeutic plant extracts such as *Syzygium aromaticum*, *Azadirachta indica*, *Embllica officinalis*, *Cinnamoum camphora*, *Avena sativa*, *etc.* were also able to produce AuNPs.<sup>11,14,15,17,18</sup>

Although widespread studies have been reported for AuNPs synthesis, systematic studies with applications are limited. In this study, we report a single step quick preparation route of AuNPs of  $\sim 38.2 \pm 10.5$  nm spherical size and stabilized *in situ* without any external capping agent using *Aegle marmelos* LE. Furthermore, these as-synthesized capped AuNPs were also used for facile detection of thiamine in aqueous solution. Thiamine or vitamin B<sub>1</sub> is a sulphur containing water soluble vitamin naturally produced in bacteria, fungi, and plants.<sup>19</sup> This vitamin enters into human or animal body from food, which is an important cofactor for many cellular processes. Thiamine deficiency causes various diseases in the human body such as beriberi, and neurological disorders, optic neuropathy, *etc.*<sup>19</sup> Additionally, it is also an essential vitamin to avoid various neurological and muscular disorders in poultry, ruminants, birds, fish, and mammals.<sup>20</sup>

A positive diagnosis of this vital vitamin in blood and tissues will help to avoid many diseases in advance, especially neurological disorders. Additionally, an easy and reliable method of detection of this essential vitamin in food and pharmaceutical industries is highly essential for different product formulations.<sup>21</sup> The widely used chemical techniques for thiamine detection are based on the reaction between chemical oxidising

Interfaces and Nanomaterials Laboratory, Department of Chemical Engineering, National Institute of Technology, Rourkela-769 008, Orissa, India. E-mail: [santanuparia@yahoo.com](mailto:santanuparia@yahoo.com); [sparia@nitrkl.ac.in](mailto:sparia@nitrkl.ac.in); Fax: +91 661 246 2999

† Electronic supplementary information (ESI) available. See DOI: 10.1039/c4ra03883e

agents and alkali, followed by the detection of fluorescent active compound thiochrome formed by oxidation reaction.<sup>22</sup> The fluorescent measurement technique is useful because of its high sensitivity, even at low concentration with less noise in the biological system; nevertheless, in other techniques such as UV-visible spectroscopy various biomolecules interfere during the analysis. Finally, numerous methods have been developed and still developing to trace out the thiamine content especially in solution phases.<sup>21,23</sup> Some research groups even used transition metal (ruthenium), and metal (cerium) mediated oxidation of thiamine, which required ~8 h incubation time with the metal catalyst for the completion of reaction.<sup>24</sup> Similarly, different chemical methodologies were reported for thiamine detection, where different special reaction conditions such as long incubation time (~16 h), elevated temperature,<sup>25</sup> and alkalinity<sup>26</sup> are required to be maintained. Nanoparticles based biosensors having good optical properties (absorption or emission) drawing significant interest in recent years.<sup>27,28</sup> However, there is no reported study available on thiamine detection using AuNPs based sensor. This study reveals that polyphenols capped AuNPs have quick oxidation ability towards thiamine to generate thiochrome (a fluorescent active compound). This sensing property of capped AuNPs towards thiamine has a huge scope to design novel sensor in bio-chemical and medical applications.

## 2 Experimental

### 2.1 Materials and methods

The chloroauric acid ( $\text{HAuCl}_4 \cdot 3.5\text{H}_2\text{O}$ ) was purchased from Loba Chemie. Potassium bromide (KBr), Sodium hydroxide (NaOH) from Merck. Ultrapure water of 18.2 mΩ cm resistivity was used throughout the study. *Aegle marmelos* LE was prepared according to our previous study.<sup>29</sup> The aqueous extract was then freeze dried to powder form (Labconco, FreeZone 2.5). A 5% stock solution of LE was prepared in deionized water and was used for the experiments.

The AuNPs were synthesized from 1 mM  $\text{HAuCl}_4$  in the presence of different concentrations of LE from 0.1–1.5% for 2 h at room temperature (~25 °C). The stoichiometric amount of LE required for the reduction reaction was determined using gold bromide complexation reaction, where the excess  $\text{HAuCl}_4$  present in solution was react with externally added KBr solution as per reaction mentioned below.<sup>30</sup>



After the completion of the reduction reaction for NPs formation, particles were separated by centrifugation and then the supernatant (1 mL) was treated with 0.3 mL of 1 N KBr solution. The gold bromide complex ( $\text{KAuBr}_4 \cdot 2\text{H}_2\text{O}$ ), was confirmed by UV-visible spectroscopy peak at 380 nm wavelength. The absence of peak indicates that the excess  $\text{HAuCl}_4$  is absent after the reaction. Additionally, kinetics of particle formation was studied by UV-visible spectroscopy which was recorded as a function of reaction time of using 1.5% LE.

To elucidate thiamine detection efficiency of the capped AuNPs, 12 μM thiamine was exposed to various concentrations of AuNPs (9.25 to 370 μg mL<sup>-1</sup>) in water : methanol (1 : 2) solutions. Then these solutions were mixed thoroughly, incubated for 20 min, the fluorescence spectra were analyzed at 425 nm wavelength, while excited at 356 nm wavelength. Furthermore, to check the particle size effect on thiamine detection efficiency, smaller size particles (~10 nm) were synthesized chemically by  $\text{NaBH}_4$  reduction using a published protocol<sup>31</sup> and then LE was added externally to adsorb on the particle surface.

### 2.2 Characterization

UV-visible spectra were recorded using a UV-visible-NIR spectrophotometer (Shimadzu, UV-3600). High-resolution transmission electron microscopy (HR-TEM, JEOL-2100F) and scanning electron microscopy (SEM, JEOL JSM 6480 LV) were used to identify the particle sizes and shapes wherever necessary. Participation of the active functional groups in the reduction process of gold precursor was identified by FT-IR spectroscopy (Bruker, USA), equipped with a horizontal attenuated total reflectance (ATR) device with zinc selenide (ZnSe) crystal. Zeta (ζ) potentials of LE and AuNPs were measured by Malvern zeta size analyser, (Nano ZS). X-ray diffraction measurements were done by Philips (PW1830 HT) X-ray diffractometer, in the range of 20–90° (2θ) at a scan rate of 0.05° s<sup>-1</sup>. Thermal gravimetric analysis (TGA) was performed using Shimadzu, DTG-60H. The changes in weight in TGA were recorded from 50 to 600 °C at a heating rate of 5 K min<sup>-1</sup>.

## 3 Results and discussion

### 3.1 Effect of leaf extract concentration on particle size

In general, identification of the stoichiometric ratio for green route synthesis is equally important as that of the wet chemical route to minimise the excess precursor during the reaction process. To identify that, the prepared LE (5.0%) was diluted to 0.1, 0.2, 0.3, 0.5, 0.7, and 1.0% solutions and exposed to 1 mM  $\text{HAuCl}_4$  for 2 h to complete the reaction. The spectral patterns because of the surface plasmon resonance (SPR) effect of AuNPs in the presence of different LE concentrations are shown in Fig. 1(a). At 0.1% LE, one can clearly see that there is no prominent peak of AuNPs. This could be because of low LE concentration which is insufficient to produce NPs. As the LE concentration increases to 0.2%, a broad peak pattern of AuNPs is observed. The presence of a shoulder type hump at 700–750 nm along with a peak at 550 nm may be because of the presence of various sizes and non-spherical shape NPs. While the concentration of LE increases to 0.3% and above, the characteristic peaks with  $\lambda_{\text{max}}$  value at ~543 nm are observed which indicates the absorption of AuNPs in the visible region of the electromagnetic spectrum.<sup>32</sup>

To find the presence of excess  $\text{HAuCl}_4$  in the reaction mixture, KBr solution was added to the supernatant after the separation of particles to form a gold complex ( $\text{KAuBr}_4 \cdot 2\text{H}_2\text{O}$ ).

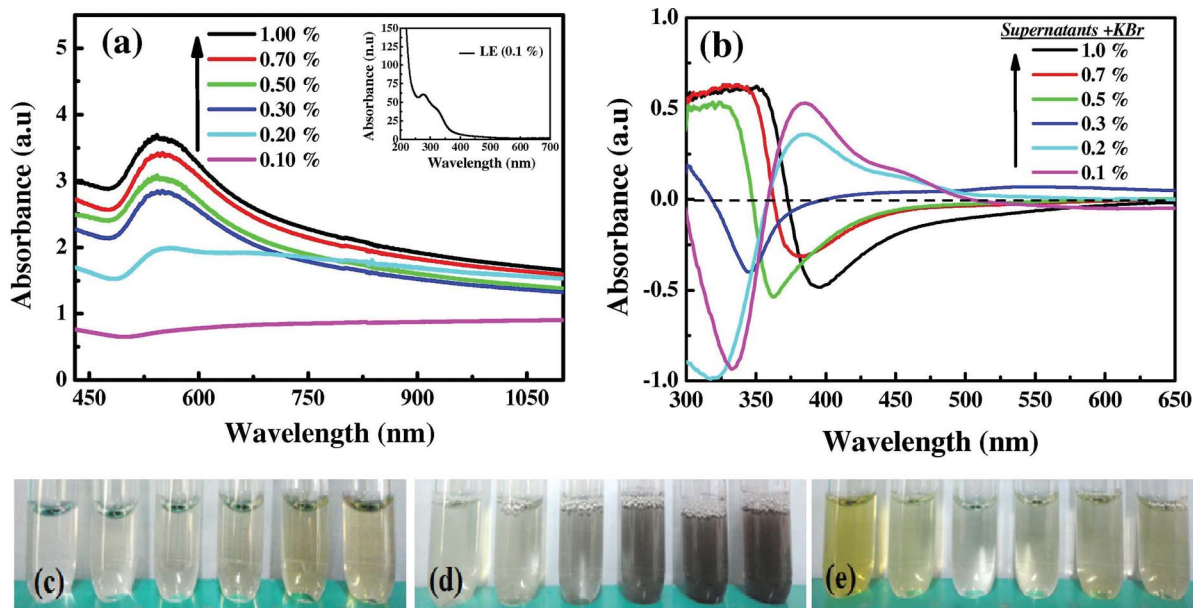


**Fig. 1** (a) UV spectra of the AuNPs after reaction with different LE concentrations (0.1–1.0%). (b) UV-Vis spectra of KBr treated supernatants after reaction with 1 mM HAuCl<sub>4</sub> and different concentrations of LE (0.1 to 1.0%). (c) Photographs of pure LE before reaction (left to right increasing concentration, 0.1 to 1.0%). (d) Colour changes of respective solutions after AuNPs formation. (e) Photographs of respective supernatants (after completion of particle formation) treated with 1 N KBr.

The complex formation was confirmed by the characteristic UV-visible peak ( $\lambda_{\text{max}}$ ) at 380 nm shown in Fig. 1(b). The physical appearances because of the colour change of different reaction systems are shown in photographs of Fig. 1(c)–(e). The absence of positive absorbance peak at 380 nm for 0.3% of LE and above in UV-visible spectra indicates no excess HAuCl<sub>4</sub> present in the reaction mixture.<sup>30</sup> Therefore, 1.0 mM/0.3% (HAuCl<sub>4</sub>/LE) concentration was taken as the stoichiometric ratio for complete reduction.

The role of LE concentration below the stoichiometric ratio on particle formation was studied further. The UV-Visible spectral pattern of AuNPs synthesized from non-stoichiometric proportion of 1.0 mM/0.2% (HAuCl<sub>4</sub>/LE) is shown in Fig. 1(a). The less intense broad spectral pattern extended towards NIR region may be because of the presence of either larger sized or non-homogenous nanoparticles. The possibility of formation of larger size particles was mainly because of the insufficient capping effect.<sup>33</sup> The molecules of LE responsible for capping effect are discussed in later sections. The as-synthesized NPs in the presence of excess HAuCl<sub>4</sub> and water washed AuNPs after removing excess HAuCl<sub>4</sub> was observed under SEM (Fig. S1†). Microscopic analysis of as-synthesized AuNPs from Fig. S1a† displays the self-assembled pattern having branches at 90° when the drop was dried on a glass surface. Interestingly, the patterned behaviour was absent when the mentioned AuNPs were separated by centrifugation and are subjected to water wash as shown in Fig. S1b.†

Self-assembled structures of AuNPs on the glass surface, shown in Fig. S1a† are because of excess residual HAuCl<sub>4</sub> upon evaporation on glass substrate under a 60 W incandescent bulb. The temperature of ~125 °C might assist in the assembled pattern of residual HAuCl<sub>4</sub> in the presence of low strength LE.

The self-assembled pattern is formed mainly at the centre of the drop (Fig. S1a†). The SEM images show that the presence of excess HAuCl<sub>4</sub> helps to form fractal type self-assembly, where branches are consist of already formed AuNPs. Thus AuNPs alone cannot form the pattern, but presence of metal salt and NPs are required for the formation of self assembly as shown by some reported study.<sup>34</sup>

### 3.2 Kinetics of particle formation

To know the equilibrium reaction time of AuNPs formation, the progress of reaction using 1.0 mM aqueous HAuCl<sub>4</sub> in the presence of 1.5% LE was monitored with time by UV-Vis spectroscopy. The absorption spectra at 543 nm wavelength ( $\lambda_{\text{max}}$ ) during the reaction at different time intervals are shown in Fig. 2(a). The rise in the maximum absorbance value is initially very fast because of the formation of AuNPs and then finally saturated after 30 min. This result indicates, ~30 min time is required for the completion of the reduction reaction. The change in absorbance as a function of time at a constant wavelength of 543 nm is shown in Fig. 2(b) and the colour change due to nanoparticles was shown in Fig. 2(c). This spectral behaviour indicates the reduction reaction and subsequent nuclei generation processes are completed within ~25 min and followed by growth.

### 3.3 XRD and electron microscopic characterization of nanoparticles

The TEM micrographs of AuNPs prepared from 1 mM HAuCl<sub>4</sub> and 1.5% LE is shown in Fig. 3(a)–(c). The particles formed in this green route are mostly spherical to little irregular shapes having almost homogeneous size distribution with

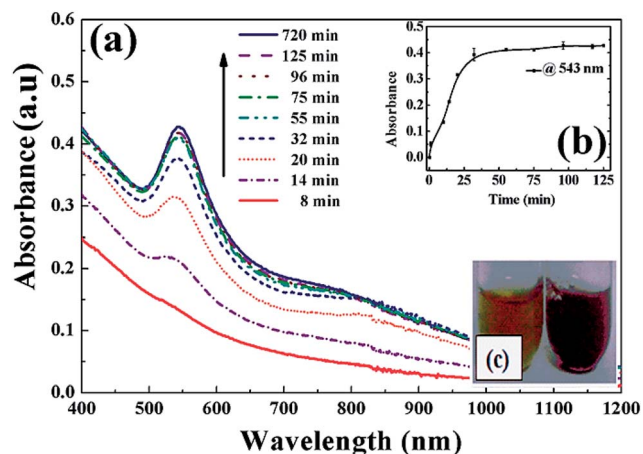


Fig. 2 (a) UV-visible spectra of AuNPs recorded with the progress of reaction time using 1.0 mM aqueous  $\text{HAuCl}_4$  and 1.5% LE (taking LE as a reference). (b) Particle growth kinetics (absorbance vs. time) at 543 nm wavelength. (c) The colour change of the LE before (left) and after the reaction (right) due to AuNPs formation.

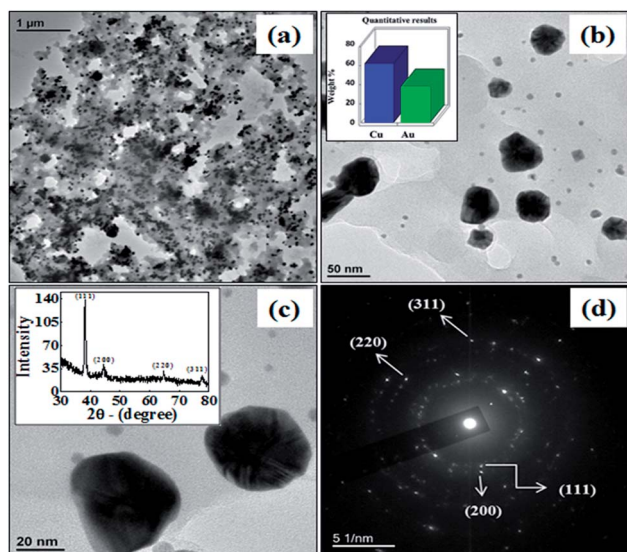


Fig. 3 (a) Low magnification TEM image of AuNPs using 1.0 mM/1.5% ( $\text{HAuCl}_4$ /LE). (b) and (c) HR-TEM images of AuNPs. Inset of (b), HRTEM-EDS analysis of the AuNPs. Inset of (c), powder XRD pattern. (d) SAED pattern of the obtained AuNPs.

an average diameter of  $\sim 38.2 \pm 10.5$  nm. Particle histograms of TEM images are given in Fig. S2.† The presence of gold was confirmed by the EDX analysis, as shown in the inset of Fig. 3(b), and the SAED pattern of AuNPs from HR-TEM (Fig. 3(d)) shows the rings corresponding to the (111), (200), (220), and (311) reflections of the face-centered-cubic (fcc) structure of Au. The crystallinity of purified AuNPs was also confirmed by the powder XRD analysis. The XRD pattern of AuNPs with  $2\theta$  peaks at  $38.20^\circ$ ,  $44.50^\circ$ ,  $64.68^\circ$ ,  $77.61^\circ$  matching with JCPDS file no: 04-0784 corresponds to the above mentioned planes and fcc structure, shown in the inset of Fig. 3(c).

### 3.4 FT-IR analysis for functional groups identification

The FT-IR spectroscopy was done in ATR mode to identify the responsible functional groups of LE in the  $\text{Au}^{3+}$  ions reduction and capping of AuNPs. Fig. 4 shows the spectra of pure LE (curve I), supernatant after reduction of Au salt (curve II), water washed AuNPs (curve III), and NaOH washed AuNPs (curve IV). The absorbance in the range of  $1500\text{--}900\text{ cm}^{-1}$  from the IR spectra of curves I and II, reveal that the characteristic of polyphenolic tannin molecules present in LE.<sup>35</sup> The pure LE shows (curve I) the peak bands at 1521, 1458, 1397, 1340, 1320, 1273, 1235, 1163, and  $1034\text{ cm}^{-1}$  which are exclusively for the presence of tannins.<sup>36</sup> Additionally, the presence of broader peaks in the regions of  $\sim 1350\text{ cm}^{-1}$  and between 1290 and  $1150\text{ cm}^{-1}$  indicate that tannins of LE are 'hydrolysable' type. These two peak regions can be assigned to C–O stretching (at  $1370\text{ cm}^{-1}$ ) and OH deformation vibrations (with absorptions at 1273, 1235 and  $1163\text{ cm}^{-1}$ ).<sup>36</sup> The presence of these molecules was also confirmed before in our previous study.<sup>29</sup>

The LE after the reduction (curve II) of  $\text{HAuCl}_4$  shows almost similar peak pattern that of curve I with few changes are as follows: a new peak appears at  $637\text{ cm}^{-1}$  and peak splitting patterns, and multiple absorptions (indicated with a star) at the peak regions of 1541, 1652 and  $1700\text{ cm}^{-1}$ . These peaks of  $\sim 1500$  and  $1600\text{ cm}^{-1}$  are because of aromatic C=C bond of the aromatic ring and peak at  $\sim 1700\text{ cm}^{-1}$  is because of isolated and exposed carbonyl groups (C=O) of LE after the reduction reaction.<sup>37</sup>

Furthermore, IR spectra of the supernatants of water and NaOH wash AuNPs are shown in curves III and IV respectively. While comparing curves I and III, significant changes in peaks are not observed, especially in the fingerprint region (peaks 1517, 1466, 1398, 1340, 1320, 1273,  $1031\text{ cm}^{-1}$ , etc.). This can be attributed to the adsorption of phenolic compounds such as tannic acid product on the surface of the water washed AuNPs.

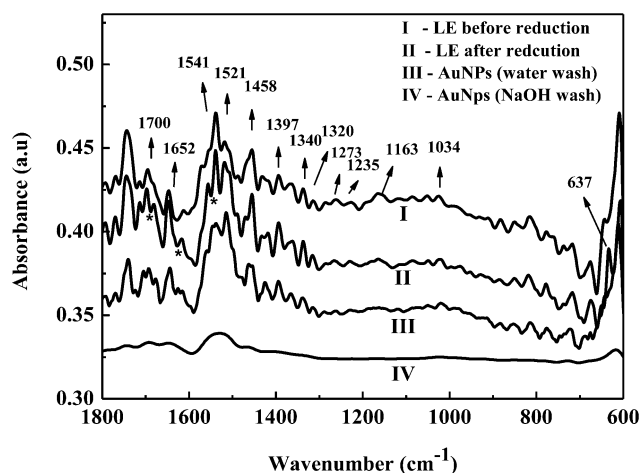


Fig. 4 ATR-FT-IR spectra of the LE (1.5%) before reduction (curve I) and after reduction (curve II) of Au salt (1.0 mM). AuNPs subjected to water wash (curve III) and NaOH wash (curve IV) also shown. Curves III, IV, represent spectrums of centrifuged, repeated water washed, dried and suspended AuNPs in deionized water.

And curve IV shows no significant peaks in the fingerprint region, which indicates the total removal of capping agent after NaOH treatment of AuNPs.

### 3.5 Tests for capping effect

FT-IR analysis indicates the presence of polyphenols in LE, which has a significant role in the gold ion reduction as well as stabilization of AuNPs because of capping. To further probe the capping ability of these molecules, synthesized AuNPs were washed with water and subsequently treated with NaOH solution, and then the supernatant solutions were analyzed by UV-visible spectroscopy. Fig. 5(a) clearly shows the absence of any distinct peak for the water wash supernatant, whereas NaOH wash supernatant shows a maximum absorbance at 276 nm; which indicates the presence of polyphenols released from AuNPs surface.

The strong adsorption ability of polyphenols onto AuNPs can also be supported by TGA analysis. The TGA analysis of pure LE, AuNPs (water and NaOH washed) are presented in Fig. 5(b). The thermal decomposition of LE – (curve I) shows majorly three zones. The first step of the transition is between 65 to 115 °C with a mass loss of 4.56%, which can be attributed to the loss of moisture and preliminary oxidation steps and elimination of volatile fractions. The second step of the transition where a weight loss of 30.43% was occurred between 115 to 354 °C, attributed to first pyrolysis step of the adsorbed molecules of

LE. Between 355 and 500 °C is the second pyrolysis step and contributes to 22.78% weight loss. Finally, above ~500 °C weight remains constant (42.23%) because of carbonized residue.<sup>38</sup>

The TGA pattern of water washed AuNPs (curve II) also shows three thermal zones similar to that of pure LE. These transitions are between 65 to 110 °C, 110 to 345 °C, and 346 to 513 °C with weight losses of 3.6, 19.6, and 26.43% respectively. However, the weight remained above ~515 °C is 50.37% because of the presence of residual carbon (due to capping agent) and AuNPs.

The TGA analysis of naked AuNPs obtained after NaOH wash (curve III) displayed no distinguished transition steps, unlike to that of curve I and II. The thermal zone appreciated between 65 to 477 °C with a mass loss of 62.11% attributes to moisture loss and/or oxidation step to eliminate the adhered volatile fractions. Finally, after heating at 477 °C the residue was 37.89% of naked AuNPs. The total weight loss calculated from curve II and III at 112 to 513 °C is 9.05%, which contributes to the weight of capping agent present in the total weight of water washed capped AuNPs.

### 3.6 Zeta potential ( $\zeta$ ) studies

The  $\zeta$  potentials of the LE solutions (before and after the reaction) and AuNPs (as-synthesized, water washed, and NaOH treated) were measured to know the presence of capping agent adsorbed on the particle surface. One can see from the Fig. S3† that all samples show negative  $\zeta$  potential. While comparing  $\zeta$  potentials,  $LE_{treat}$  shows a slight lower potential than  $LE_{fresh}$  because of the absence of some active tannin molecules and the presence of extra  $H^+$  ions from  $HAuCl_4$ . Further, the negative  $\zeta$  potential values of AuNPs show the following order: within  $LE < water\ wash < NaOH\ wash$ . The pattern observed is mainly because of capping effect of tannin molecules on the surface of the AuNPs. Repeated water wash NPs show more negative value than that in pure LE because of the removal of loosely bound tannin molecules, and NaOH wash particles show highest  $\zeta$  potential value because of complete removal of the adsorbed molecules from the particle surface. The observed  $\zeta$  potential value after NaOH wash ( $-42.9 \pm 2.45$  mV) is close to the reported value of pure AuNPs which are around  $\sim -41$  to 44 mV at neutral pH.<sup>39,40</sup> Moreover, it has also been found that the  $\zeta$  potential value of repeated methanol washed AuNPs is  $-42.4 \pm 1.9$  mV is close to that of NaOH wash (Fig. S3†). So the adsorbed phenolic compounds can also be removed by repeated methanol wash too.

### 3.7 Capped AuNPs as thiamine sensors

A solution of 12  $\mu M$  of thiamine was added to different concentrations polyphenols capped AuNP suspensions (9.25, 27.75, 46.25, 92.50 and 185  $\mu g\ mL^{-1}$ ) in a mixture of water : methanol (1 : 2) solutions and mixed thoroughly. The final mixtures were then excited at 356 nm wavelength (excitation spectra shown in Fig. S4a†), and the respective emission spectra were measured as shown in Fig. 6. From the figure, it is very clear that the emission spectra are very prominent for all

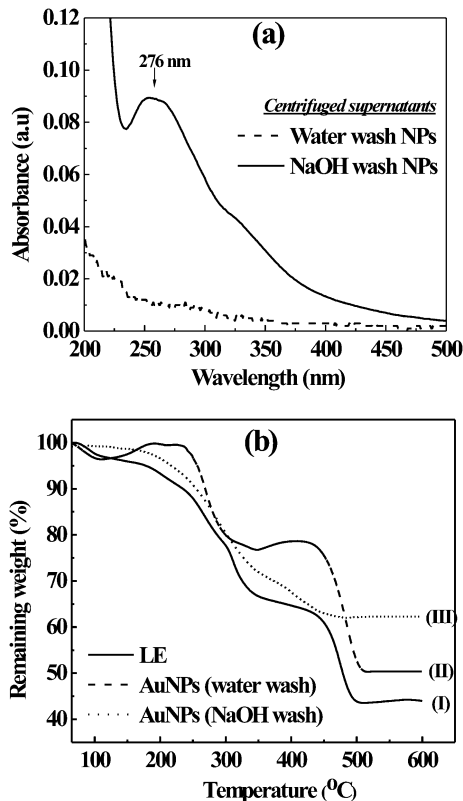


Fig. 5 (a) UV-visible absorbance spectra of supernatants of water washed and NaOH (0.5 M) treated AuNPs. (b) TGA of pure LE, AuNPs after water wash and NaOH wash.

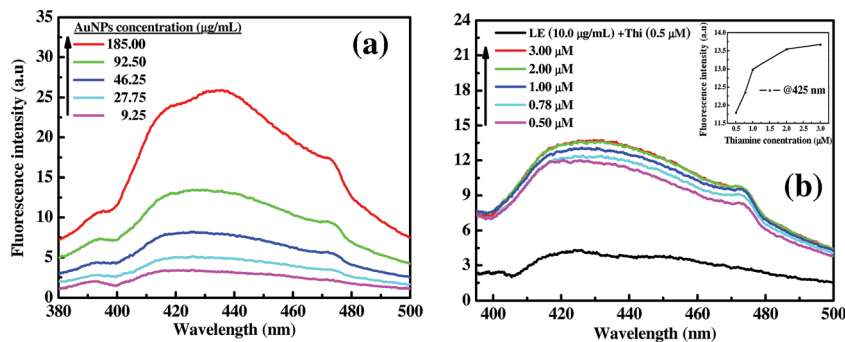


Fig. 6 (a) Fluorescence spectra of thiamine (Thi) 12  $\mu\text{M}$  with tannin capped AuNPs from  $\sim 9.25$  to  $185.0 \mu\text{g mL}^{-1}$  concentrations. (b) Spectra of thiamine (0.5 to  $3.0 \mu\text{M}$ ) exposed to  $92.5 \mu\text{g mL}^{-1}$  capped AuNPs and insert of (b) displays the fluorescence signal at fixed  $\lambda_{\text{emi}}$  of 425 nm with respect to increase in thiamine concentration. Fluorescence signal spectrum devoid of AuNPs with only capping agent ( $10.0 \mu\text{g mL}^{-1}$ ) exposed to thiamine ( $0.5 \mu\text{M}$ ) is also shown in (b).

different doses of AuNPs and the intensity increases linearly at  $\lambda_{\text{max}}$  of 425 nm with increasing concentration of AuNPs dose.

Furthermore, Fig. 6(b) also shows intense fluorescent peaks with varying thiamine concentrations (0.5 to  $3.0 \mu\text{M}$ ) for a constant dose of AuNPs ( $92.5 \mu\text{g mL}^{-1}$ ). From the figure it can be observed that a constant spectral pattern for 2.0 and  $3.0 \mu\text{M}$  thiamine concentrations, and this infers that there is a maximum level of the detection limit ( $2 \mu\text{M}$ ) for a particular dose of capped AuNPs ( $92.5 \mu\text{g mL}^{-1}$ ). This behaviour may be because of the unavailability of the capping agent for thiamine oxidation. The fluorescence signal pattern at  $\lambda_{\text{max}}$  (425 nm) clearly indicates the threshold level of thiamine detection is about  $\sim 1.5 \mu\text{M}$  by  $92.5 \mu\text{g mL}^{-1}$  of AuNPs dose (Fig. 6(b) insert). It is also interesting to observe that the fluorescence signal was enhanced by the use of AuNPs in combination with capping agent which is responsible for the thiamine oxidation. When the only LE equivalent to that associated with  $92.5 \mu\text{g mL}^{-1}$  AuNPs *i.e.*  $\sim 10.0 \mu\text{g mL}^{-1}$  (revealed from TGA analysis) was individually exposed to thiamine ( $0.5 \mu\text{M}$ ), an emission intensity of 4.2 at 425 nm wavelength was observed; which is  $\sim 3.5$  times lower than the capped AuNPs of  $92.5 \mu\text{g mL}^{-1}$  (Fig. 6(b)). The fluorescence signal detection by pure LE devoid of AuNPs also followed a linear pattern as shown in Fig. S4b.†

To see the importance of *in situ* capping by LE polyphenols and effect of particles size on thiamine detection,  $\sim 10$  nm AuNPs were synthesized chemically and tested. The AuNPs were synthesized by  $\text{NaBH}_4$  reduction method<sup>31</sup> and incubated with LE for the adsorption of polyphenols. The particles were separated, used for thiamine detection, and emission spectra are shown in Fig. S5.† It has been found that the detection signal is significantly lower compared to that of *in situ* synthesized particles. In this case, although the particle size is low, polyphenol adsorption or capping effect is also low, which in turn reduce the detection efficiency. Less adsorption of polyphenols was also confirmed by the  $\zeta$  potential measurements. The observed  $\zeta$  potential values for AuNPs prepared by borohydrate method are  $-26$  mV (as-prepared) and  $-30.9$  mV (after water wash). From the  $\zeta$  potential and fluorescence results, we can say that the stabilization effect by LE molecules towards AuNPs is

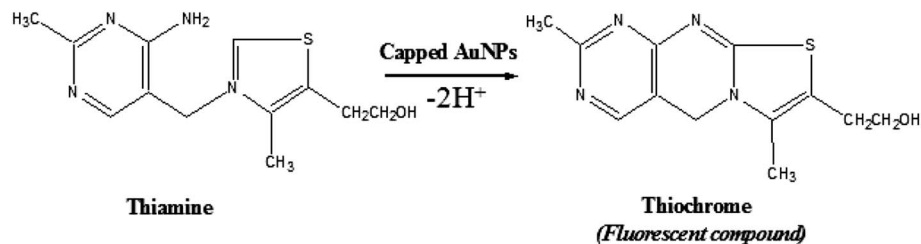
stronger for *in situ* synthesis, and which is also essential for the detection of thiamine. The enhancement of fluorescence intensity in the presence of capped AuNPs is attributed to the behavior of distance dependent fluorescence resonance electron transfer (FRET).<sup>41</sup> In general; AuNPs are excellent FRET-based quenchers because of their extraordinary high extinction coefficient and broad energy absorption bandwidth in the visible region.<sup>42</sup> Usually in quenching effect, initially a donor fluorophore absorbs the energy due to the excitation of incident light and transfer the excitation energy to a nearby acceptor chromophore (here AuNPs).



In this case, generally two fluorophores (donor and acceptor) must be in the close proximity to one another. The intensification in fluorescence signal is observed after thiamine oxidation by capped AuNPs, which is a reverse behaviour of quenching effect. The signal enhancement is acceptable as the particle and fluorophore are separated by capping agent which in turn reduced the quenching effect and probably enhanced the rate of fluorescence decay.<sup>41</sup>

As the AuNPs surface is well capped by polyphenols of LE, it is possible to maintain this distance easily to get FRET. The signal enhancement is highly advantageous for the development of high sensitive thiamine sensors. It is also worthy to note that only pure thiamine or naked AuNPs in the presence of thiamine ( $12 \mu\text{M}$ ) exhibited no significant fluorescent peak at 425 nm (Fig. S6a†) indicates the absence of thiochrome generation. The process of thiamine oxidation by capped AuNPs is illustrated in Scheme 1.

The detection procedure is novel because of the simplicity of the process, detection at neutral pH without long incubation time. This simple procedure of thiamine detection at ambient condition was not possible by the reported chemical routes,<sup>20,21,24</sup> and our study shows better detection efficiency



Scheme 1 Schematic illustration of thiamine oxidation by capped AuNPs.

than the reported studies, which are able to detect minimum thiamine concentration in the range of 100,<sup>22</sup> ~86.4,<sup>21</sup> and 50  $\mu\text{M}$ <sup>24</sup> effectively.

Further, as a supporting evidence, we also investigated the structural changes of thiamine (20  $\mu\text{M}$ ) by UV-visible spectroscopic study (Fig. S6b†) after the addition of capped AuNPs (2.32 mg mL<sup>-1</sup>). The UV spectrum of thiamine usually exhibits two distinct absorption maxima at neutral pH and a merged appearance at acidic pH.<sup>23</sup> Fig. S6b† shows UV absorption spectra before exposure to capped AuNPs with two distinct absorption peaks characteristic of pure thiamine at 241 and 259 nm wavelengths at pH ~6.0 which in accordance with a reported study.<sup>23</sup> These  $\lambda_{\text{max}}$  values shifted to 234 and 267 nm wavelengths after addition of capped AuNPs, attributed to the oxidation of the thiazole ring of thiamine. It has been also found that the reaction time for the conversion of thiamine in the presence of capped AuNPs to its oxidized product thiochrome (specified in fluorescent results) is instantaneous. The structural changes in amine functional group of thiamine are clearly evident after oxidation process and visible shifts in the IR absorption region of  $\sim 3400\text{ cm}^{-1}$  was also observed (ESI, Fig. S7† dotted region). From the figure, peaks at 3489 and 3423  $\text{cm}^{-1}$  (because of absorption by primary amine) were replaced by a single peak at 3427  $\text{cm}^{-1}$  (because of the secondary amine) after oxidation of thiamine.

## 4 Conclusions

In conclusion, we demonstrated a simple, one-pot, economical and fast green approach to synthesize AuNPs of  $\sim 38\text{ nm}$  size within 30 min. A stoichiometric proportion of LE (0.3%) to  $\text{HAuCl}_4$  (1 mM) was established for complete reduction process. The HR-TEM and XRD analysis shows the spherical shape and crystalline fcc structure of the formed AuNPs. Apart from reduction process, *in situ* capping effect of polyphenolic molecules (tannins) of LE on AuNPs was also supported by FT-IR spectroscopy, UV-vis spectroscopy, TGA, and zeta potential studies. The sensing capability of capped AuNPs towards thiochrome (an oxidative product of thiamine) by fluorescence spectroscopy shows  $\sim 0.5\ \mu\text{M}$  or below thiamine concentration can be easily detected by a minimum nanoparticle dose of 92.50  $\mu\text{g mL}^{-1}$ . We strongly believe these results are useful for the synthesis of bio-compatible polyphenols capped AuNPs, which can be further applicable for sensing of thiamine. The produced

AuNPs (with or without capping) also be used in other applications, as well.

## References

- G. J. Hutchings, A golden future for green chemistry, *Catal. Today*, 2007, **122**, 196–200.
- R. Luque, R. S. Varma, J. H. Clark and G. A. Kraus, *Sustainable Preparation of Metal Nanoparticles: Methods and Applications*, Royal Society of Chemistry, 2012.
- K. N. Thakkar, S. S. Mhatre and R. Y. Parikh, Biological synthesis of metallic nanoparticles, *Nanomedicine*, 2010, **6**, 257–262.
- J. A. Dahl, B. L. S. Maddux and J. E. Hutchison, Toward greener nanosynthesis, *Chem. Rev.*, 2007, **107**, 2228–2269.
- J. H. Clark, Green chemistry: challenges and opportunities, *Green Chem.*, 1999, **1**, 1–8.
- A. K. Jha, K. Prasad, K. Prasad and A. R. Kulkarni, Plant system: nature's nanofactory, *Colloids Surf., B*, 2009, **73**, 219–223.
- S. Girija, Y. L. Balachandran and J. Kandakumar, Plants as green nanofactories: application of plant biotechnology in nanoparticle synthesis – A review, *Plant Cell Biotechnol. Mol. Biol.*, 2009, **10**, 79–86.
- D. A. Giljohann, D. S. Seferos, W. L. Daniel, M. D. Massich, P. C. Patel and C. A. Mirkin, Gold nanoparticles for biology and medicine, *Angew. Chem., Int. Ed.*, 2010, **49**, 3280–3294.
- M. C. Daniel and D. Astruc, Gold nanoparticles: assembly, supramolecular chemistry, quantum-size-related properties, and applications toward biology, catalysis, and nanotechnology, *Chem. Rev.*, 2004, **104**, 293–346.
- N. A. Begum, S. Mondal, S. Basu, R. A. Laskar and D. Mandal, Biogenic synthesis of Au and Ag nanoparticles using aqueous solutions of black tea leaf extracts, *Colloids Surf., B*, 2009, **71**, 113–118.
- D. Raghunandan, M. D. Bedre, S. Basavaraja, B. Sawle, S. Manjunath and A. Venkataraman, Rapid biosynthesis of irregular shaped gold nanoparticles from macerated aqueous extracellular dried clove buds (*Syzygium aromaticum*) solution, *Colloids Surf., B*, 2010, **79**, 235–240.
- W. Liang, T. L. Church and A. T. Harris, Biogenic synthesis of photocatalytically active Ag/TiO<sub>2</sub> and Au/TiO<sub>2</sub> composites, *Green Chem.*, 2012, **14**, 968.
- M. Noruzi, D. Zare and D. Davoodi, A rapid biosynthesis route for the preparation of gold nanoparticles by aqueous

- extract of cypress leaves at room temperature, *Spectrochim. Acta, Part A*, 2012, **94**, 84–88.
- 14 A. K. Mittal, Y. Chisti and U. C. Banerjee, Synthesis of metallic nanoparticles using plant extracts, *Biotechnol. Adv.*, 2013, **31**, 346–356.
  - 15 O. V. Kharissova, H. V. R. Dias, B. I. Kharisov, B. O. Pérez and V. M. J. Pérez, The greener synthesis of nanoparticles, *Trends Biotechnol.*, 2013, **31**, 240–248.
  - 16 N. A. Begum, S. Mondal, S. Basu, R. A. Laskar and D. Mandal, Biogenic synthesis of Au and Ag nanoparticles using aqueous solutions of black tea leaf extracts, *Colloids Surf., B*, 2009, **71**, 113–118.
  - 17 S. S. Shankar, A. Rai, A. Ahmad and M. Sastry, Rapid synthesis of Au, Ag, and bimetallic Au core–Ag shell nanoparticles using neem (*Azadirachta indica*) leaf broth, *J. Colloid Interface Sci.*, 2004, **275**, 496–502.
  - 18 V. Armendariz, I. Herrera, J. R. Peralta-vidua, M. Joseyacamán, H. Troiani, P. Santiago and J. L. Gardea-Torresdey, Size controlled gold nanoparticle formation by *Avena sativa* biomass: use of plants in nanobiotechnology, *J. Nanopart. Res.*, 2004, **6**, 377–382.
  - 19 G. F. Combs Jr, *The Vitamins*, Academic Press, 2007.
  - 20 A. F. Makarchikov, B. Lakaye, I. E. Gulyai, J. Czerniecki, B. Coumans, P. Wins, T. Grisar and L. Bettendorff, Thiamine triphosphate and thiamine triphosphatase activities: from bacteria to mammals, *Cell. Mol. Life Sci.*, 2003, **60**, 1477–1488.
  - 21 P. L. López-de-Alba, L. López-Martínez, V. Cerdá and J. Amador-Hernández, Simultaneous determination and classification of riboflavin, thiamine, nicotinamide and pyridoxine in pharmaceutical formulations, by UV-visible spectrophotometry and multivariate analysis, *J. Braz. Chem. Soc.*, 2006, **17**, 715–722.
  - 22 M. Fujiwara and K. Matsui, Determination of thiamine by thiochrome reaction, *Anal. Chem.*, 1953, **25**, 810–812.
  - 23 S. Y. Reddy, R. Pullakhandam and B. Dinesh Kumar, Thiamine reduces tissue lead levels in rats: mechanism of interaction, *BioMetals*, 2009, **23**, 247–253.
  - 24 K. S. Byadagi, D. V. Naik, A. P. Savanur, S. T. Nandibewoor and S. A. Chimatadar, Ruthenium(III) mediated oxidation of thiamine hydrochloride by cerium(IV) in perchloric acid medium: a kinetic and mechanistic approach, *React. Kinet., Mech. Catal.*, 2010, **99**, 53–61.
  - 25 K. Gold, Some factors affecting the stability of thiamine, *Limnol. Oceanogr.*, 1968, **13**, 185–188.
  - 26 H. K. Penttinen, Differences in thiochrome fluorescence produced by thiamine and its mono-, di-, and triphosphate esters, *Acta Chem. Scand.*, 1976, **30**, 659–663.
  - 27 K. L. Kelly, E. Coronado, L. L. Zhao and G. C. Schatz, The optical properties of metal nanoparticles: the influence of size, shape, and dielectric environment, *J. Phys. Chem. B*, 2002, **107**, 668–677.
  - 28 M. Mandal, N. R. Jana, S. Kundu, S. K. Ghosh, M. Panigrahi and T. Pal, Synthesis of Au core–Ag shell type bimetallic nanoparticles for single molecule detection in solution by SERS method, *J. Nanopart. Res.*, 2004, **6**, 53–61.
  - 29 K. Jagajjanani Rao and S. Paria, Green synthesis of silver nanoparticles from aqueous *Aegle marmelos* leaf extract, *Mater. Res. Bull.*, 2013, **48**, 628–634.
  - 30 A. K. Gangopadhyay and A. Chakravorty, Charge transfer spectra of some gold(III) complexes, *J. Chem. Phys.*, 1961, **35**, 2206–2209.
  - 31 M. P. Mallin and C. J. Murphy, Solution-phase synthesis of sub-10 nm Au–Ag alloy nanoparticles, *Nano Lett.*, 2002, **11**, 1235–1237.
  - 32 T. Sakai and P. Alexandridis, Single-step synthesis and stabilization of metal nanoparticles in aqueous pluronic block copolymer solutions at ambient temperature, *Langmuir*, 2004, **20**, 8426–8430.
  - 33 P. R. Sajanlal, T. S. Sreepasad, A. K. Samal and T. Pradeep, Anisotropic nanomaterials: structure, growth, assembly, and functions, *Nano Rev.*, 2011, **2**, 5883.
  - 34 N. N. Jason, R. Ghosh Chaudhuri and S. Paria, Selfassembly of colloidal sulfur particles influenced by sodium oxalate salt on glass surface from evaporating drops, *Soft Matter*, 2012, **8**, 3771–3780.
  - 35 L. Falcão and M. E. M. Araújo, Tannins characterization in historic leathers by complementary analytical techniques ATR-FTIR, UV-vis and chemical tests, *J. Cult. Herit.*, 2013, **14**, 499–508.
  - 36 L. Laghi, G. P. Parpinello, D. D. Rio, L. Calani, A. U. Mattioli and A. Versari, Fingerprint of enological tannins by multiple techniques approach, *Food Chem.*, 2010, **121**, 783–788.
  - 37 J. Coates, *Interpretation of Infrared Spectra, a Practical Approach*, Wiley Online Library, 2000.
  - 38 M. A. Pantoja-Castro and H. González-Rodríguez, Study by infrared spectroscopy and thermogravimetric analysis of tannins and tannic acid, *Rev. Latinoam. Quím.*, 2011, **39**, 107–112.
  - 39 S. Park, M. Park, P. Han and S. Lee, The effect of pH-adjusted gold colloids on the formation of gold clusters over APTMS-coated silica cores, *Bull. Korean Chem. Soc.*, 2006, **27**, 1341–1345.
  - 40 T. Kim, C.-H. Lee, S.-W. Joo and K. Lee, Kinetics of gold nanoparticle aggregation: experiments and modeling, *J. Colloid Interface Sci.*, 2008, **318**, 238–243.
  - 41 K. A. Kang, J. Wang, J. B. Jasinski and S. Achilefu, Fluorescence manipulation by gold nanoparticles: from complete quenching to extensive enhancement, *J. Nanobiotechnol.*, 2011, **9**, 16.
  - 42 P. C. Ray, A. Fortner and G. K. Darbha, Gold nanoparticle based FRET assay for the detection of DNA cleavage, *J. Phys. Chem. B*, 2006, **110**, 20745–20748.